45th AIAA Aerospace Sciences Meeting and Exhibit AIAA-2007-586
Reno, Nevada, 8-11 January 2007

High Power Ion Cyclotron Heating In the VASIMR Engine

Edgar A. Bering, III[1]
University of Houston, Departments of Physics and ECE, Houston, TX 77204, USA

Franklin R. Chang-Díaz[2], Jared P. Squire[3], Verlin Jacobson[4], and Leonard D. Cassady[5]
Ad Astra Rocket Company, Mail code: ASPL, 2101 NASA Parkway, Houston, TX 77058, USA

and

Michael Brukardt[6]
University of Houston, Departments of Physics, Houston, TX 77204, USA

The Variable Specific Impulse Magnetoplasma Rocket (VASIMR) is a high power magnetoplasma rocket, capable of Isp/thrust modulation at constant power. The plasma is produced by a helicon discharge. The bulk of the energy is added by ion cyclotron resonance heating (ICRH.) Axial momentum is obtained by adiabatic expansion of the plasma in a magnetic nozzle. Thrust/specific impulse ratio control in the VASIMR is primarily achieved by the partitioning of the RF power to the helicon and ICRH systems, with the proper adjustment of the propellant flow. Ion dynamics in the exhaust were studied using probes, gridded energy analyzers (RPA's), microwave interferometry and optical techniques. This paper will review high power single-pass ICRH ion acceleration data, with emphasis on the most recent results.

Nomenclature

η_A	=	ICRH antenna efficiency
η_b	=	ion coupling efficiency
f	=	frequency
f_{ci}	=	ion cyclotron frequency
F	=	ion velocity phase space distribution function
Γ_i	=	total ion flux
I_{sp}	=	specific impulse
L_A	=	inductance of the ICRH antenna
L_M	=	inductance of the ICRH antenna matching network
m_{doti}	=	mass flow rate
P_{plasma}	=	ICRH RF power broadcast into plasma
P_{ion}	=	ICRH RF power coupled into ions
P_{ICRH}	=	ICRH RF power into antenna
Q_c	=	quality factor of the ICRH antenna coupling circuit
R_c	=	resistance of the ICRH antenna coupling circuit
R_p	=	plasma loading of the ICRH antenna
Θ	=	pitch angle
v_{ICRF}	=	exhaust plasma flow velocity with ICRH on
$v_{helicon}$	=	exhaust plasma flow velocity with helicon only

[1] Professor, Physics and ECE, 617 Science & Research I / PHYS 5005, Associate Fellow.
[2] Chief Executive Officer, Ad Astra Rocket Company, Mail code: ASPL, 2101 NASA Parkway, Associate Fellow.
[3] Director of Research, Ad Astra Rocket Company, Mail code: ASPL, 2101 NASA Parkway, Member
[4] Staff Scientist, Ad Astra Rocket Company, Mail code: ASPL, 2101 NASA Parkway
[5] Lead Project Engineer, Ad Astra Rocket Company, Mail code: ASPL, 2101 NASA Parkway, Student Member
[6] Research Assistant, Physics, Professor, 617 Science & Research I / PHYS 5005

$VSWR_{plasma}$ = voltage standing wave ratio of the ICRH antenna, with plasma present
$VSWR_{vacuum}$ = voltage standing wave ratio of the ICRH antenna, with no plasma present
W_{ICRH} = mean ion energy increase owing to ICRH
ω = angular frequency

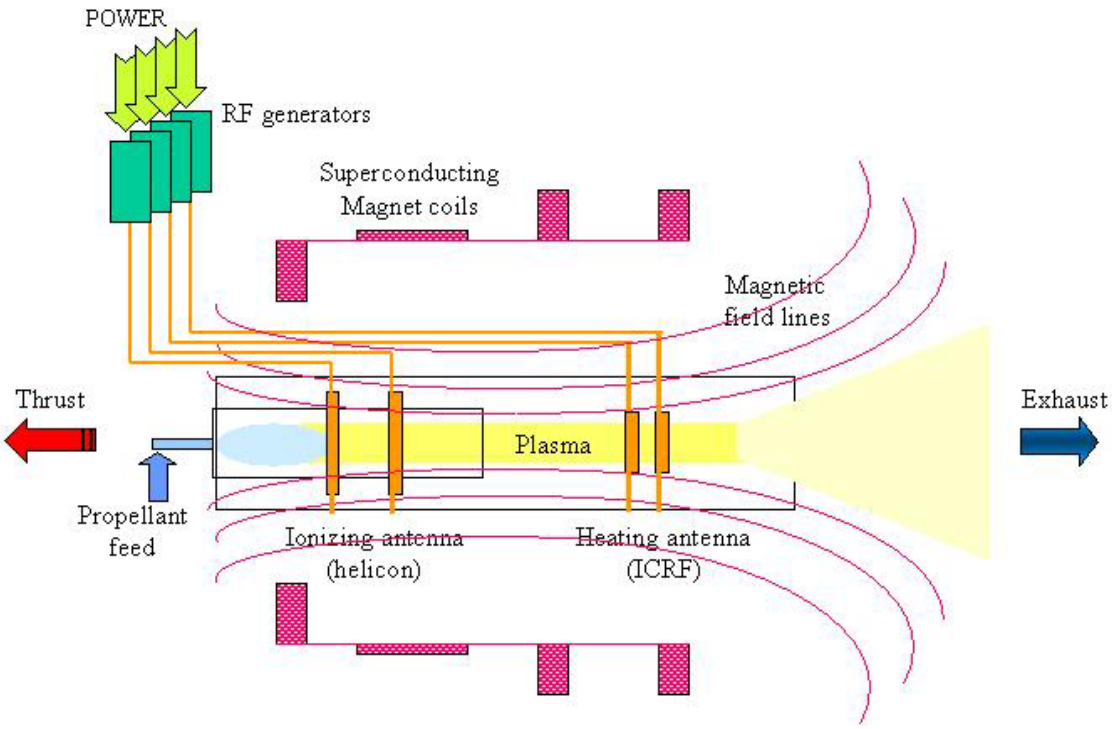

Figure 1. Cartoon block diagram of the VASIMR system, illustrating the basic physics.

I. Introduction

THE exploration of the solar system will be one of the defining scientific tasks of the new century. One of the obvious challenges faced by this enterprise is the scale size of the system under study, 10^{11} - 10^{14} m. Over distances on this scale and given the performance of present day rockets, the mission designer is faced with the choice of accepting multi-year or even decadal mission time lines, paying for enormous investment in rocket propellant compared to useful payload, or finding a way to improve the performance of today's chemical rockets. For human space flight beyond Earth's orbit, medical, psychological, and logistic considerations all dictate that drastic thruster improvement is the only choice that can be made. Even for robotic missions beyond Mars, mission time lines of years can be prohibitive obstacles to success, meaning that improvements in deep space sustainer engines are of importance to all phases of solar system exploration[1]. Improvement in thruster performance can best be achieved by using an external energy source to accelerate or heat the propellant[2,3]. This paper will discuss an experimental investigation of the use of Ion Cyclotron Resonance Heating (ICRH) to provide an efficient method of electrodeless plasma acceleration in the VAriable Specific Impulse Magnetoplasma Rocket (VASIMR) engine.

Research on the VASIMR engine began in the late 1970's, as a spin-off from investigations on magnetic divertors for fusion technology[4]. A simplified schematic of the engine is shown in Figure 1. The VASIMR consists of three main sections: a helicon plasma source, an ICRH plasma accelerator, and a magnetic nozzle[3,5,6,7,8,9]. Figure 1 shows these three stages integrated with the necessary supporting systems. One key aspect of this concept is its electrode-less design, which makes it suitable for high power density and long component life by reducing plasma erosion and other materials complications. The magnetic field ties the three stages together and, through the magnet assemblies, transmits the exhaust reaction forces that ultimately propel the ship.

The plasma ions are accelerated in the second stage by ion cyclotron resonance heating (ICRH), a well-known technique, used extensively in magnetic confinement fusion research[10,11,12,13,14]. Owing to magnetic field limitations on existing superconducting technology, the system presently favors the light propellants; however, the helicon, as a stand-alone plasma generator can efficiently ionize heavier propellants such as argon and xenon.

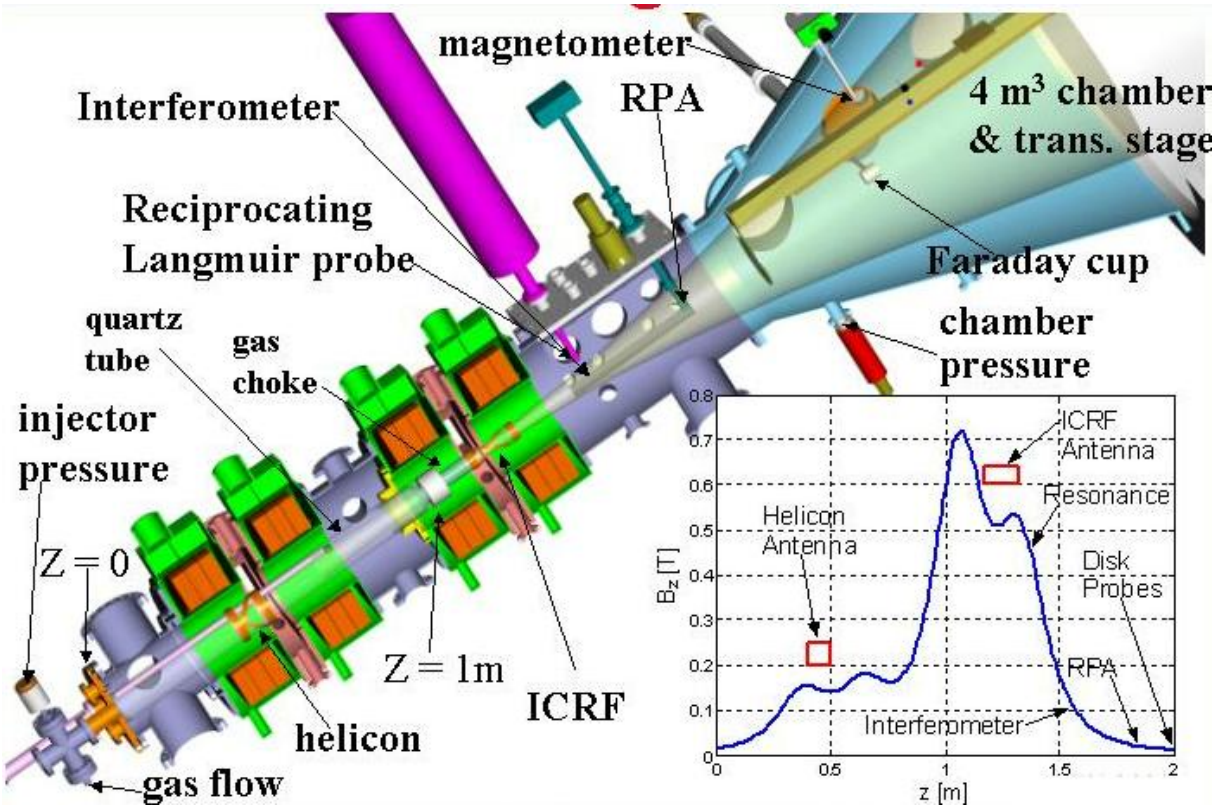

Figure 2. Cutaway trimetric engineering drawing of the present configuration of the VASIMR VX-50.

An important consideration involves the rapid absorption of ion cyclotron waves by the high-speed plasma flow. This process differs from the familiar ion cyclotron resonance utilized in tokamak fusion plasmas as the particles in VASIMR pass under the antenna only once[9,15,16,17]. Sufficient ion cyclotron wave (ICW) absorption has nevertheless been predicted by recent theoretical studies[18], as well as observed and reported in various conferences and symposia.

Elimination of a magnetic bottle, a feature in the original VASIMR concept, was motivated by theoretical modeling of single-pass absorption of the ion cyclotron wave on a magnetic field gradient[18]. While the cyclotron heating process in the confined plasma of fusion experiments results in approximately thermalized ion energy distributions, the non-linear absorption of energy in the single-pass process results in a boost, or displacement of the ion kinetic energy distribution. The ions are ejected through the magnetic nozzle before thermal relaxation occurs.

Natural processes in the auroral region also exhibit ICRH. Single-pass ICRH ion acceleration has been invoked to explain observations of "ion conic" energetic ion pitch angle distributions in the auroral regions of the Earth's ionosphere and magnetosphere[19,20,21,22,23,24,25]. The fact that ion conics are commonly found on auroral field lines suggests that ICRH is a ubiquitous process in auroral arcs. The efficiency of the wave-particle coupling that single pass heating can produce is illustrated by the fact that space-borne observations of ion-cyclotron waves are relatively rare[26,27,28,29,30,31,32,33,34].

This paper presents the data from a series of experiments that have conclusively demonstrated single pass ICRH in a fast-flowing laboratory plasma. The paper will emphasize the results from recent experiments where 10's of kW of ICRH power have been available.

II. Experiment

A. The VASIMR Engine

The VASIMR engine has three major subsystems, the plasma generator stage, the RF "booster" stage and the nozzle, shown in Figures 1 and 2[8]. A laboratory physics demonstrator experiment (VX-50), was developed and tested at the NASA Johnson Space Center and more recently at the Ad Astra Rocket Company for several years[35,36]. The details of the engine and its design principles have been previously reported[9,37]. The first stage is a helicon discharge that has been optimized for maximum power efficiency (lowest ionization cost in eV/(electron-ion

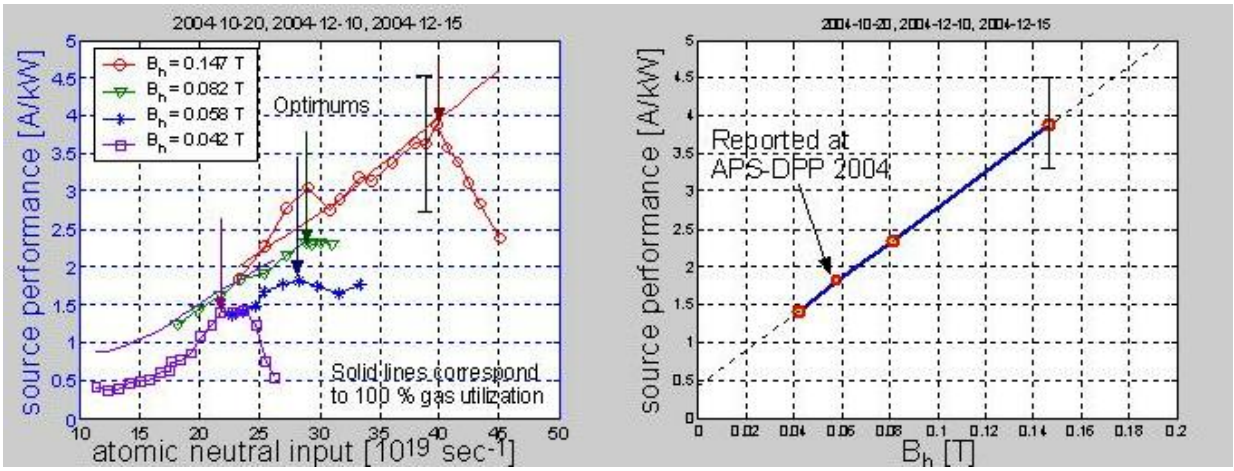

Figure 3. (a) Source performance is plotted vs. gas flow rate for 4 different values of the helicon magnetic field strength. (b) Source performance vs. magnetic field strength.

pair)[38,39,40,41]. The next stage downstream is the heating system. Energy is fed to the system in the form of a circularly polarized rf signal tuned to the ion cyclotron frequency. ICRH heating has been chosen because it transfers energy directly and largely to the ions, which maximizes the efficiency of the engine[11,12]. In the present small-scale test version, there is no mirror chamber and the ions make one pass through the ICRH antenna. The system also features a two-stage magnetic nozzle, which accelerates the plasma particles by converting their azimuthal energy into directed momentum. The detachment of the plume from the field takes place mainly by the loss of adiabaticity and the rapid increase of the local plasma β, defined as the local ratio of the plasma pressure to the magnetic pressure.

The main VASIMR vacuum chamber is a cylinder 1.8 m long and 35.6 cm in diameter. The VASIMR exhaust flows through a conical adapter section into a 5 m^3 exhaust reservoir. The magnetic field is generated by four liquid nitrogen cooled 150 turn copper magnets, which can generate a magnetic induction of up to 1.5 T. The high vacuum pumping system consists of a cryopump and two diffusion pumps with a combined total capacity of 5000 l/s.

Prior to the investigations reported here, there have been a series of improvements and upgrades to the helicon plasma source[42,43,44]. The earliest experiments[3,15] were performed using a 5 cm diameter ``Boswell'' type double saddle antenna and 3 kW of rf power. Directionality was provided by use of a magnetic cusp configuration. Over the next 3.5 years[43,44], the helicon underwent a number of successive upgrades. The helicon plasma source in the VASIMR engine was incrementally improved in three steps. First, antenna size, connector and power supply improvements raised the available power from 3 kW to 10 kW, still operating with Boswell antenna and a magnetic cusp. The factors limiting the application of rf power to the helicon ionizing discharge had been the power of the 25

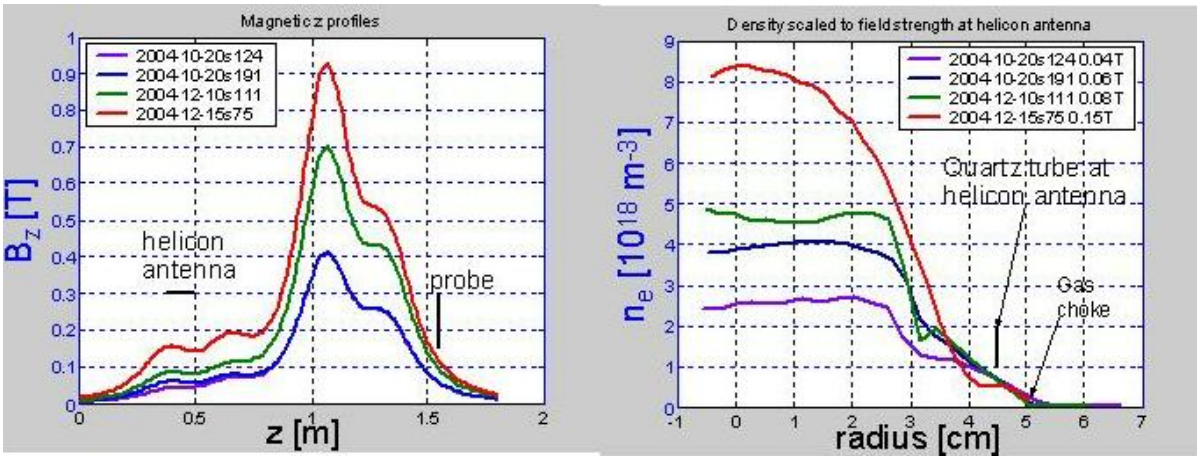

Figure 4. (a) Magnetic field profiles for the four configurations in Figure 3. (b) Density profiles as a function of radius for the 4 configurations.

MHz transmitter (3 kW), the voltage limits on the vacuum rf feed-through, the voltage limits of the rf matching network and the diameter of the discharge. Successive steps to 9 cm increased the diameter of the helicon antenna. The helicon rf supply was completely rebuilt. A new high voltage power supply was built, along with a new high power transmitter. A 10 kV rf vacuum feed-through was obtained and installed, along with a new high voltage matching network. These new components produced helium plasma operating at 10 kW, with ~4 times the ion flux achievable at 3 kW. Second, the transmitting antenna was changed from the Boswell configuration to a helical half-twist antenna. Finally, the decision was taken to switch transmitters and power the helicon with our 100 kW transmitter, which can operate the helicon at 13.5 MHz. A high voltage (30 kV) water-cooled vacuum feed-through was manufactured to enable full power operation. In all configurations, the vacuum feed-through and helicon antennas were water cooled and capable of steady state operation.

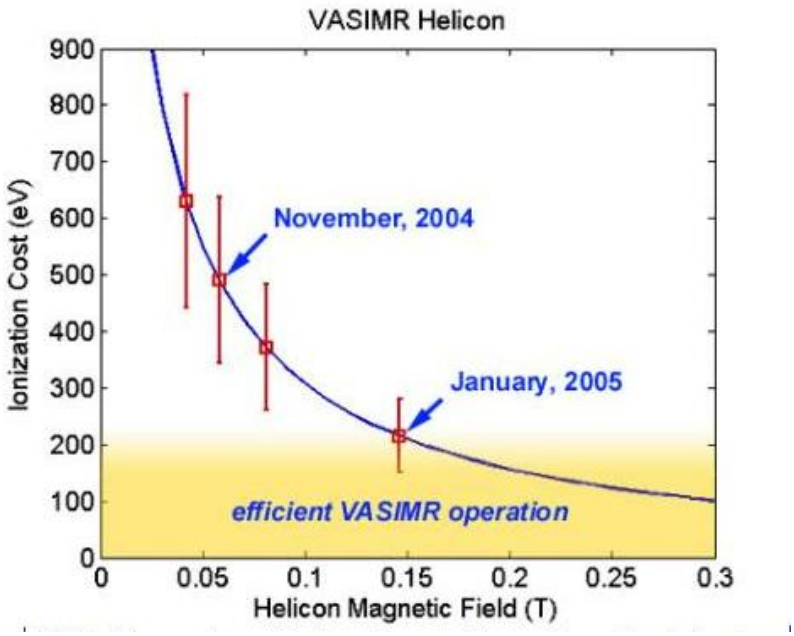

Figure 5. Ionization cost in eV/ion pair is shown as a function of helicon magnetic field strength.

The ICRH antenna is a helical, double strap quarter-turn antenna configuration. It is polarized to launch left-handed slow mode waves[16,45]. The present configuration of the rf booster or ICRH system uses 1.5-3. MHz left hand polarized slow mode waves launched from the high field, over dense side of the resonance (region 13 of the Clemmow-Mullaly-Allis (CMA) diagram, using the Stix[14] notation). The antenna was uncooled, which limits the pulse length to typically less than 0.5 s. The pulse power was limited by the rf power source to 1.5 kW until 2006.

ICRH power levels up to 30 kW are described in this paper. A new ICRH transmitter was installed at the end of 2005. During 2006, experiments studying the application of high power ICRH to dense flowing plasma were performed[46]. This paper will focus on the RPA data in order to describe these experiments and highlight some of the experimental results that have been obtained. We explored the details of the ion dynamics in deuterium, neon and argon exhaust plasma using 20 kW of RF power to the helicon ionization stage and 20-30 kW to the ICRH acceleration stage. We have demonstrated a further increase in booster efficiency and begun exploring the parameter space that this additional power has opened up. In particular, we have begun to explore the dependence of specific impulse on input gas flow rate.

B. Diagnostics

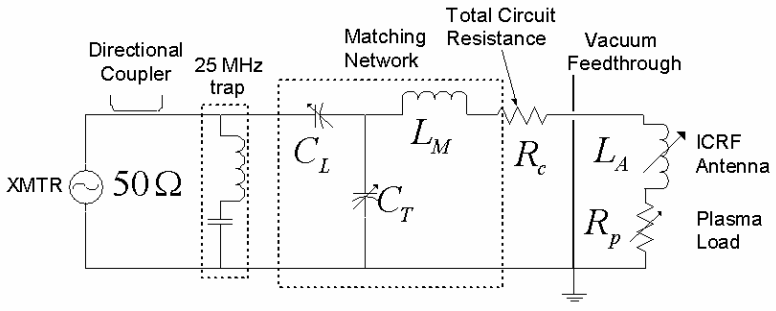

Figure 6. Circuit diagram of the ICRH antenna, indicating how the plasma impedance couples to the circuit.

Available plasma diagnostics include a triple probe, 32 and 70 GHz density interferometers, a bolometer, a television monitor, an H-α photometer, a spectrometer, neutral gas pressure and flow measurements, several gridded energy analyzers (retarding potential analyzer or RPA)[3,8,47,48,49,50,51,52,53], a momentum flux probe, an emission probe, a directional, steerable RPA and other diagnostics[54]. Reciprocating Langmuir[55] and

density interferometer are the primary plasma diagnostics. The Langmuir probe measures ion current and temperature profiles and is calibrated by the density interferometer. An array of thermocouples provides a temperature map of the system. The Langmuir probe has four molybdenum tips that are biased as a triple probe, with an extra tip for measuring electrostatic fluctuations[55].

1. Retarding potential analyzer (RPA)

Retarding potential analyzer (RPA) diagnostics have been installed to measure the accelerated ions. The present RPA is a planar ion trap located ~40 cm downstream from the plane of the triple probe, which corresponds to a factor of 8 reduction in the magnetic field strength. The grids are 49.2-wire/cm nickel mesh, spaced 1 mm apart with Macor spacers. The opening aperture is 1 cm in diameter, usually centered on the plasma beam. A four-grid configuration is used, with entrance attenuator, electron suppressor, ion analyzer and secondary suppressor grids.

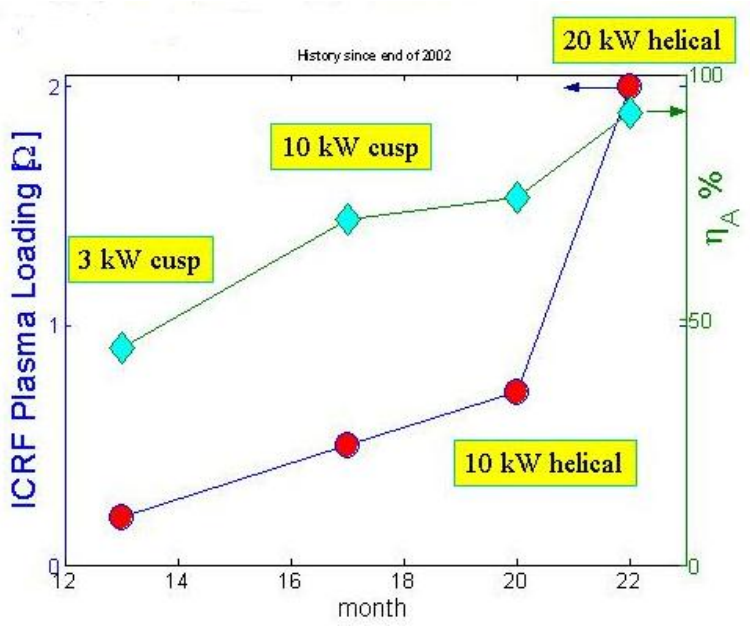

Figure 7. ICRF Plasma loading plotted as a function of month since January 2003

The interpretation of RPA output data in terms of ion energy requires an accurate knowledge of plasma potential (V_p). When available, data from an rf compensated swept Langmuir probe provided by Los Alamos National Laboratory (LANL) are used to determine V_p. When other V_p data are not available, plasma potential is assumed to be the value at which *dI/dV* first significantly exceeds 0, which usually agrees with the LANL probe value within the error bars. This value is typically ~+30-50 V with respect to chamber ground. The operator biases the body and entrance aperture of the RPA to this value. The ion exhaust parameters are deduced from the raw data by means of least squares fits of drifting Maxwellians to the current-voltage data[48,50,53,56].

C. Ionization Investment

During the interval from May 2004 to March 2004, a major part of the experimental effort was devoted to the parameter space of the helicon injector in an effort to improve efficiency and reduce ionization costs. Between May 2004 and the present, the source performance was improved by roughly an order of magnitude. The source performance has doubled since the AIAA meeting in January 2005, as shown in Figure 3. The performance appears proportional to the applied magnetic field at the helicon antenna, at least in this range, as shown in Figures 3 and 4. Start up problems and feedthrough arcing prevented us from going to higher fields. The energy cost per ion pair has been reduced to ~ 200 eV/ion pair at gas utilization approaching 100%. These values are competitive with most other high power electric thrusters, and will enable the VASIMR as a whole to achieve competitive efficiencies.

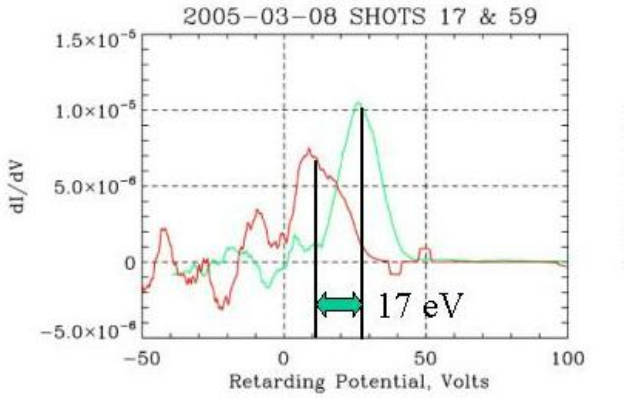

Figure 8 Ion energy distribution comparing ICRH on and off conditions, illustrating ion acceleration by ICRH.

Four magnetic field profiles with which we performed a gas flow scan at about 20 kW are shown in Figure 4. Note the very large density increase at high magnetic field. The density profiles are all scaled to the helicon antenna field strength, for comparison. The density at the helicon antenna is likely much higher, since the flow velocity is high (supersonic) at the probe. The helicon

operating frequency was almost 5 times the LH resonance frequency during the maximum performance runs.

The history of ionization cost is plotted as a function of helicon magnetic field strength in Figure 5. We are very close to our goal for the helicon, < 200 eV/ion-electron pair. Further improvements appear possible.

D. Plasma Loading

The light ion VASIMR engine is best suited to high power operation. The critical factor that limits efficiency at low power is the efficiency of helicon stage and hence the ionization cost[57]. At high power, the ICRH stage is more important and hence ICRH antenna loading is more critical here. The load impedance of the antenna must be significantly larger than the impedance of the transmission and matching network (see Figure 6). The cyclotron resonance frequency of helium in the available magnetic field is about 2 MHz, which means that one requires plasma that is ~8-10 centimeters in diameter before reasonable load impedances are obtained.

The following calculation illustrates how plasma loading is determined. The analysis begins with the relationship that:

$$\frac{VSWR_{plasma}}{VSWR_{vacuum}} = \frac{R_p + R_c}{R_c} \tag{1}$$

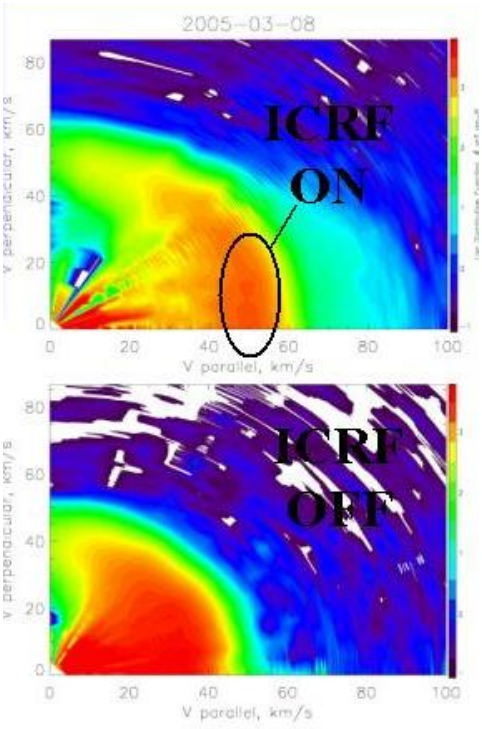

Figure 9. Ion velocity phase space distribution functions, comparing low power (1.5 kW) ICRH on and off conditions.

where VSWR is the Voltage Standing Wave Ratio. A network analyzer is used in place of the high power rf transmitter to measure the quality factor (Q_c) of the antenna coupling circuit and to tune the circuit when no plasma is present. With measuring the impedance matching (L_m) and the antenna inductances (L_m and L_A , respectively), we have:

$$R_c = \frac{\omega\left(L_m + L_A\right)}{Q_c} \approx 0.24\ \Omega \tag{2}$$

and

$$R_p = R_c\left(VSWR_{plasma} - 1\right). \tag{3}$$

Thus, the coupling efficiency is:

$$\eta_A = \frac{R_p}{\left(R_p + R_c\right)} = 0.89 \tag{4}$$

and the power radiated into the plasma is estimated as:

$$P_{plasma} = \eta_A P_{ICRH} = 1.25\ \text{kW}. \tag{5}$$

The initial deuterium loading data were taken when only 4 kW of helicon power was available. Plasma loading was generally maximum when $f/f_{ci} > 1$. The plasma loading was comparable to the circuit resistance. Helium data showed similar behavior. More recent loading measurements have been made using a 20 kW helicon discharge. The

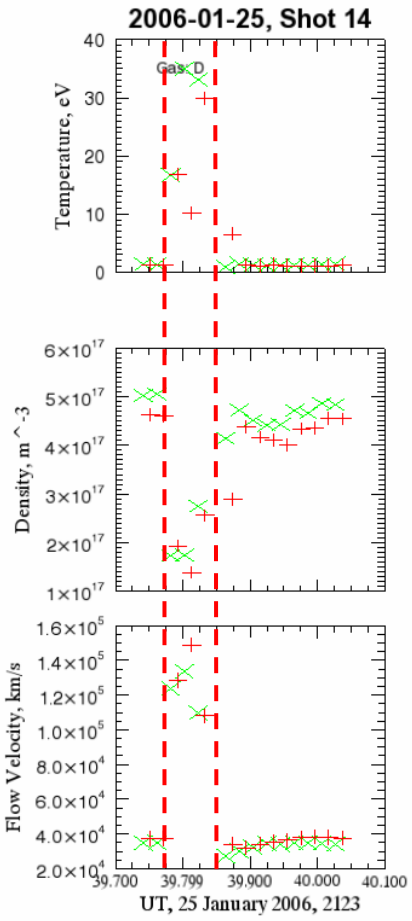

Figure 10. Fit parameters obtained by least squares fitting a drifting Maxwellian representation to each voltage sweep obtained by the wide angle RPA during a pulsed ICRH deuterium plasma shot. From bottom to top, the panels show ion drift velocity, ion density and ion temperature in the frame of the beam. The plusses and X's show up and down sweeps. The vertical dashed lines show the times when the ICRH turned on and off.

measurements show very good loading, ~2 Ω, which implies a corresponding high coupling efficiency, as shown in Figure 7. This high loading impedance was obtained with a sizable, ~1 cm, plasma-antenna gap. Maximum in the loading occurred at f/f_{ci} = 0.95, indicating that the antenna was launching a more propagating wave than it was in the low-density case.

III. Ion Cyclotron Resonance Heating (ICRH)

A. Deuterium, 1.5 kW ICRH

In January 2004, we reported ICRH data taken with only a 4 kW helicon deuterium discharge. ICRH power was only 1.4 kW. Ion kinetic energy data were taken on-axis with an RPA and emissive LP. Energy boosts of over 160 eV were observed. We have since increased plasma fluxes over an order of magnitude. With that same ICRH power, we expect energy boosts of about 20 eV with the higher fluxes. Recently, we have performed a series of experiments to measure the ICRH energization with the higher density plasma. We observed clear acceleration with with ICRH. The observed energy boost was 17 eV, more than double the energy with the helicon alone, as shown in Figures 8 and 9. Two-dimensional contour plots of the ion velocity phase space distribution functions that were obtained by rotating the RPA, shot-to-shot[58,59], are shown in Figure 9. Evidence of pitch angle scattering by neutrals may be seen in both panels of Figure 9. The change in the distribution function corresponds to a 0.55 density drop, consistent with simultaneous interferometer data.

B. Deuterium, 20 kW ICRH

Starting in January, 2006, a 100 kW ICRH transmitter was installed on the VASIMR VX-50 demonstration experiment. As a practical matter, applied ICRH power was initially limited to ~20 kW by the voltage limits on the vacuum feed-through and by the fact that the ICRH antenna is uncooled. A series of high-power ICRH experiments was performed on deuterium plasma produced by a helicon discharge operating between 13 and 25 kW of input RF power. Four sets of experiments were performed, including scans of ICRH input power for two gas flow rate and helicon power combinations, a scan of the discharge profile at the axial location of the RPA and observations of the pitch angle dependence of the ion velocity phase space distribution function for both the ICRH off and ICRH on condition at high power.

The fact that the ICRH transmitting antenna was uncooled limited us to pulsed ICRH operations during this series of experiments. Typically 0.1 to 0.4 s pulses were used. An example of the results of this procedure is shown in Figure 10. This Figure shows the parameters inferred by fitting the current-voltage (I-V) characteristic that would be produced by a drifting Maxwellian ion distribution to the raw RPA data. In Figure 10, each RPA sweep that was recorded during a particular shot has been separately fit to a Maxwellian and the results plotted as time series as shown in the Figure. The X's and plusses show different signs of the of the retarding potential sweep slope. During the shot shown in Figure 10, the operating gas was deuterium, which was flowing in at a rate of 450 standard cubic centimeters per minute (sccm). 20 kW of RF power at 13.56 MHz drove the helicon discharge. 20 kW of RF power at 3 MHz was supplied to the ICRH antenna. The ICRH quadrupled the bulk flow speed of the ions, from ~35 km/s to~140 km/s. The density did not quite fall by a factor of 4, which indicates that the ICRH produced additional ionization in the plasma. This result is a consequence of using an unoptimized helicon discharge, which happened to have too high a gas flow for the available helicon power to fully ionize. In contrast to our results at 1,5 kW of ICRH power, at 20 kW the ion temperature in the frame

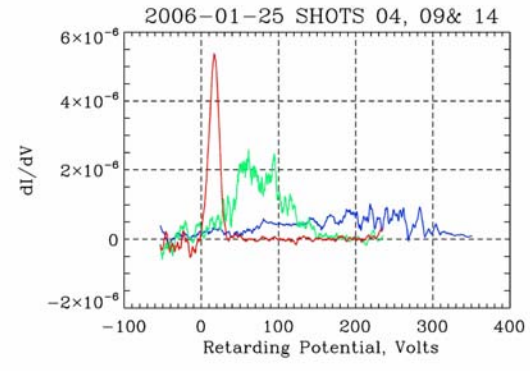

Figure 11. The first derivative of the current-voltage characteristics measured by an RPA with 30º collimation oriented at 0º pitch angle in a series of deuterium plasma shots. The lowest energy, red curve shows a shot without ICRH, the medium energy, darker curve shows a shot with 8.3 kW of ICRH, and the high energy, blue curve shows a shot with 20 kW of ICRH.

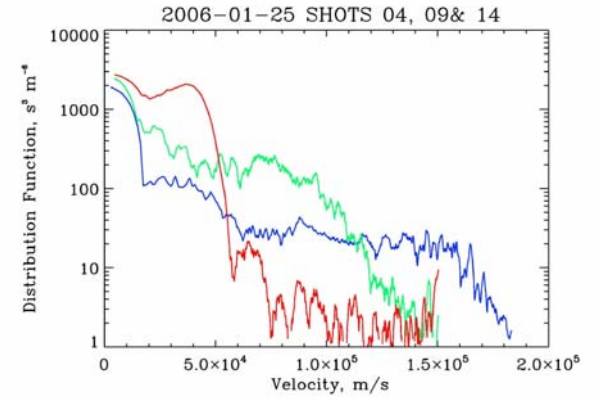

Figure 12. The ion velocity phase space distribution functions inferred from the data shown in Fig. 11.

of the beam increases by nearly 2 orders of magnitude, which indicates that there are processes acting to thermalize the plasma.

Figure 11 shows a comparison of the first derivative of the characteristic curve obtained by the wide aperture RPA during helium plasma shots run with 0, 8.3 and 20 kW of ICRH power. The elevated multi-peaked sections between 50 and 130 eV in the 8.3 kW data and 50 and 300 eV in the 20 kW data are indicative of the presence of a population of strongly heated ions. The presence of what appear to be hot components with low drift velocity is attributed to the fact that we have not yet been able to afford to obtain sufficient vacuum pumping capacity for this experiment. Consequently the background pressure builds up to at least 20 microtorr in the 50 cm region between the ICRH antenna and the RPA during the period of the discharge when RPA data were taken. The data show exactly the expected signature. The velocity phase space distribution functions corresponding to Figure 11 are found by dividing by the energy and are shown in Figure 12. The differences between the three curves appear less dramatic in this logarithmic presentation. Nonetheless, the effect of significant particle heating is apparent.

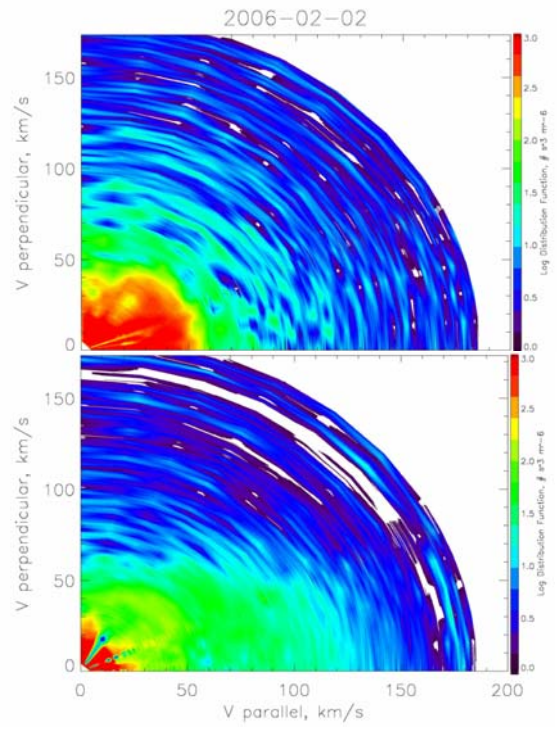

Figures 13, 14. Same as Figure 9 showing the ion velocity phase space distribution function for ICRH-off (Figure 13, top) and 14 kW of ICRH (figure 14, bottom).

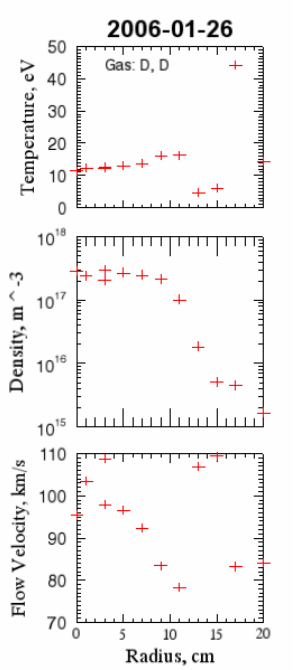

Figure 15. Fit parameters obtained by least squares fitting drifting Maxwellians to RPA data taken while scanning the radial location of the RPA. Each symbol represents the average of all sweeps during a single shot.

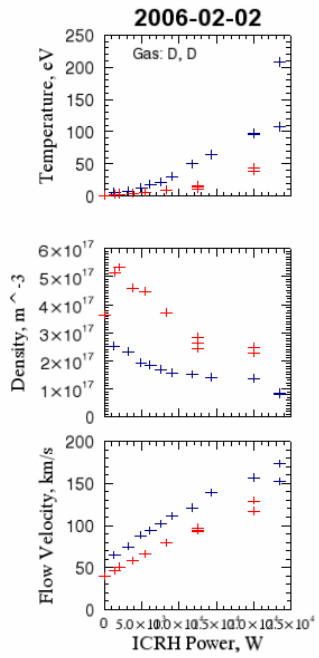

Figure 16. Fit parameters obtained by least squares fitting drifting Maxwellians to RPA data taken while scanning the ICRH power. Each symbol represents the average of all sweeps during a single shot. Red symbols correspond to a deuterium flow rate of 450 sccm and a helicon input power of 20 kW. The blue symbols correspond to a flow rate of 250 sccm and 17 kW of helicon power.

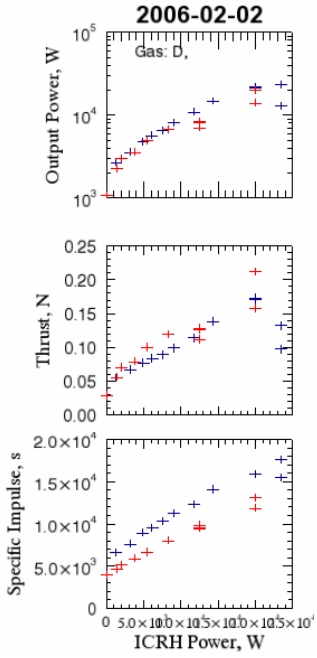

Figure 17. Rocket performance parameters inferred by integrating the data of Figure 16 over a uniform disk of the observed 10 cm plasma radius, as shown in Figure 15 for the high flow rate (red) case. An 8 cm disk was used for the low flow rate (blue) case.

Full ion velocity phase space distribution functions can be obtained by rotating the RPA, shot-to-shot[58,59]. Two dimensional color contour plots of a planar cut through the distribution function are shown in Figure 13 for ICRH-off and Figure 14 for 14 kW of ICRH-on. Since a pitch angle of 90º at the location of the maximum field intensity maps to a pitch angle of ~10º at the location of the RPA, all of the ions in both distributions that have pitch angles >10º have been scattered, presumably by an ion-neutral collisions. There is a clear, visible difference between the two distributions, indicating that the ICRH has accelerated the entire plasma. The ICRH-on distribution shows a clear signature of a collimated jet of ions with parallel speeds as high as 150 km/s. The reduction in the maximum value of the distribution function in the ICRH on case corresponds to a density drop that was consistent with the results of simultaneous interferometer observations.

The next example of an ICRH experiment that will be presented is a radial scan of the RPA during 14 kW ICRH-on conditions. The results have been interpreted using a single Maxwellian and are shown in Figure 15. This experiment was performed with a 20 kW helicon antenna discharge and 450 sccm deuterium gas flow. Under these conditions, the plasma loading of the ICRH antenna was 2 Ω, resulting in an increase in antenna efficiency to 0.89, as shown in Figure 7. These results can be integrated to estimate the output power and momentum flux in the exhaust plume. The figure shows that the density and flow velocity profiles are essentially constant over a disk with

a radius of ~10 cm at the axial distance of the probe. The total ion flow rate was determined by the triple and RF compensated Langmuir probes, which have a more accurate absolute calibration than the RPA.

Absorption efficiency was high enough to suggest the possibility that the ion cyclotron wave was fully damped prior to reaching the center of the plasma column. This situation was investigated by means of the radial scan. Figure 15 indeed shows a small drop in bulk flow velocity and corresponding increase in ion density in the innermost 1 cm of the plasma column. This hole would indicate that 14 kW is insufficient signal strength to fully illuminate the discharge that the experiment was producing.

The Maxwellian model analysis method has been used to interpret the results of a series of shots that scanned the ICRH power input from 0-23 kW. These experiments were performed at two different gas flow/ helicon power combinations, 450 sccm/ 20 kW and 250 sccm / 17 kW. The intent was to begin to explore the variation of specific impulse that may be obtained through use of power reallocation throttling schemes in a flight model. These results are presented in Figures 16 and 17. In the figures, the high and flow rate results are shown as red and blue X's, respectively. These results further strengthen the overall result of this paper, that the VASIMR VX-50 experiment is showing convincing evidence of single pass ICRH heating and that high power ICRH encountered any problems that might act to limit ICRH RF field strength.

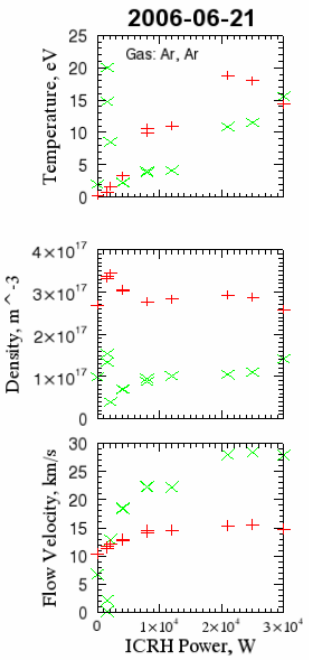

Figure 18. Argon plasma fit parameters obtained by least squares fitting drifting bi-Maxwellians to RPA data taken while scanning the ICRH power. Each symbol represents the average of all sweeps during a single shot. Red symbols correspond to a slow hot component, and green symbols correspond to a fast, cold component.

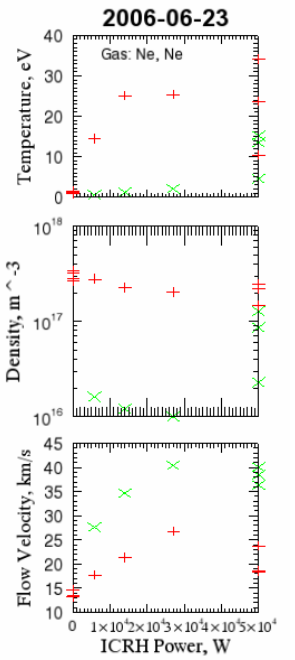

Figure 19. Neon plasma fit parameters obtained by least squares fitting drifting bi-Maxwellians to RPA data taken while scanning the ICRH power. Each symbol represents the average of all sweeps during a single shot. Red symbols correspond to a slow hot component, and green symbols correspond to a fast, cold component.

The bottom panel of Figure 16 shows the dependence of inferred bulk flow velocity on applied ICRH power. The data in this panel indicate that the lower gas flow rate discharge was accelerated to a significantly higher exhaust velocity than the high flow rate plasma, as expected. The flow speeds achieved were impressive, with speeds > 100 km/s obtained even in the high flow case. The middle panel shows the inferred densities. The high flow rate densities were significantly higher, as expected. The high flow rate case shows an increase in density occurred as the first few kW of ICRH were applied. This result is suggests that the unoptimized helicon discharge was not fully ionizing the incoming propellant, and that some of the ICRH power was contributing to fully ionizing the gas. It is also apparent that the velocity-density product was not constant in either case. This variation could be interpreted as suggesting that an increase in ion flux with increasing ICRH power occurred over the entire power range. However, such an interpretation is incorrect. What appears to have happened is that the increased flow velocity acted to stretch the magnetic field lines in the exhaust plume and reduce the radius of the plasma column. The radius of the discharge in the low flow case was only 8 cm at the RPA location at the 23 kW ICRH power level.

The low ICRH power points in the top panel show that the unaccelerated plasma has a low temperature in its reference frame, consistent with the expected output temperature of the helicon discharge. The ICRH does not heat the exhaust plasma very much until the ICRH power exceeds 15 kW in the higher flow rate case. In the low flow rate case; significant increase in the rest frame temperature of the flowing ion beam was observed above 5 kW of ICRH power.

Figure 17 shows interpretation of the data in Figure 16. The bottom panel shows the specific impulse I_{sp}, which was computed from the data in Figure 16 by simple division by g. The middle and top panels show the predicted thrust and output power computed by integrating the observations in Figure 16 over the area of the exhaust plume,

assuming a uniform radial profile as shown in Figure 15. The thrust is higher for the low flow situation, as expected. The high flow case achieved a predicted thrust of 0.19±0.02 N at 20 kW. The output power prediction in the top panel includes heat flux and chemical potential transport in the computation, which contributes < 1kW to the estimate. Since the two curves overlay, the lower total power low flow case was more efficient, achieving an apparent booster efficiency of ~90% and a total power efficiency of ~60% at 20 kW of ICRH power.

C. Neon and Argon, 30 kW ICRH

The results obtained from ICRH experiments using argon and neon as the working gasses are shown in Figures 18 and 19. The effect of resonant charge exchange with the accumulating neutral back pressure is evident in these data. The ion energy distributions show the clear presence of two components, a hot slow component, and a cold, faster component. We attribute the hot slow component to the effects of resonant charge exchange on the plasma. The pumping capacity problem that is the cause of this phenomenon will be addressed in the coming year.

The cold, fast component had maximum flow velocities of 40 and 30 km/s (4000 and 3000 s of I_{sp}) for neon and argon, respectively, at 30 kW of ICRH in. The hot component velocities exhibited a clear square root dependence on input power, as expected. Until the pumping capacity is increased, it will not be meaningful to estimate predicted thrust or efficiency.

IV. Summary

We have demonstrated acceleration of a dense ($>10^{19}/m^3$) plasma flow using ICRH in a single-pass mode, using deuterium. ICRH loading measurements are consistent with efficient (90%) coupling to the plasma, primarily ICW. The ICRH experiments have demonstrated that an energy boost of over 160 eV is possible, with no sign of limitations yet. Recent experiments have shown an ICRH acceleration efficiency of as much as 90%. Maximum predicted thrust of 0.19 N using deuterium plasma with 40 kW of RF power has been suggested by the results. 20 kW in our 9 cm diameter helicon has enabled us to raise the magnetic field and proportionally increase the plasma source efficiency to nearly 4 A/kW.

Acknowledgments

NASA Johnson Space Center under grant NAG 9-1524, the Texas Higher Education Coordinating Board under Advanced Technology Program project 003652-0464-1999 and the Ad Astra Rocket Company sponsored this research.

References

[1] K. Sankaran, L. Cassady, A. D. Kodys et al., "A survey of propulsion options for cargo and piloted missions to Mars." Presented at the *International Conference on New Trends in Astrodynamics,* Jan. 20-22, 2003 (unpublished).

[2] F. R. Chang-Díaz, "Fast, power-rich space transportation, key to human space exploration and survival." Presented at the *53rd International Astronautical Congress / The World Space Congress,* 10-19 Oct 2002, Houston, Texas, 2002.

[3] E. A. Bering III, F. R. Chang-Díaz, and J. P. Squire, "Use of RF waves in space propulsion systems, The" *Bulletin of Radio Science (310),* 92-106 (2004).

[4] F. R. Chang-Díaz and J. L. Fisher, "A supersonic gas target for a bundle divertor plasma." *Nuclear Fusion 22*(8), 1982.

[5] F. R. Chang Díaz, "Research status of the Variable Specific Impulse Magnetoplasma Rocket," presented at the *39th Annual Meeting of the Division of Plasma Physics,* 1997 (unpublished).

[6] F. R. Chang Díaz, "Research Status of the Variable Specific Impulse Magnetoplasma Rocket," presented at the *Open Systems,* July 27-31, 1998, Novosibirsk, Russia, 1998 (unpublished).

[7] F. R. Chang Díaz, J. P. Squire, A. V. Ilin et al., "Development of the VASIMR Engine, The," presented at the *International Conference of Electromagnetics in Advanced Space Applications,* Sep 13-17, 1999, Torino, Italy, 1999 (unpublished).

[8] F. R. Chang Díaz, J. P. Squire, E. A. Bering III et al., "VASIMR Engine Approach to Solar System Exploration, The," presented at the *39th AIAA Aerospace Sciences Meeting and Exhibit,* Jan. 8-11, 2001, Reno, NV, 2001.

[9] F. R. Chang Díaz, J. P. Squire, T. Glover et al., "VASIMR Engine: Project Status and Recent Accomplishments, The," presented at the *42nd AIAA Aerospace Sciences Meeting and Exhibit,* Reno, NV, 2004.

[10] N. J. Fisch, "Confining a tokamak plasma with rf-driven currents," *Physical Review Letters, 41*(13), 873 (1978).

[11] S. N. Golovato, K. Brau, J. Casey et al., "Plasma Production and Heating in a tandem mirror central cell by radio frequency waves in the ion cyclotron frequency range," *Phys. Fluids, 3* (12), 3744-3753 (1988).

[12] Y. Yasaka, R. Majeski, J. Browning et al., "ICRF heating with mode control provided by a rotating field antenna," *Nuclear Fusion, 28,* 1765 (1988).

[13] D.G. Swanson, *Plasma Waves* (Academic Press, Boston, 1989).

[14] T. H. Stix, *Waves in Plasma* (American Institute of Physics, New York, NY, 1992).
[15] E. A. Bering III, M. Brukardt, F. R. Chang-Díaz et al., "Experimental studies of the exhaust plasma of the VASIMR engine." Presented at the *40th AIAA Aerospace Sciences Meeting and Exhibit,* Reno, NV, 2002.
[16] E. A. Bering III, M. S. Brukardt, W. A. Rodriguez et al., "Ion Dynamics and ICRH Heating in the Exhaust Plasma of The VASIMR Engine." Presented at the *53rd International Astronautical Congress / The World Space Congress,* 10-19 Oct., Houston, Texas, 2002.
[17] D. G. Chavers and F. R. Chang-Díaz, "Momentum flux measuring instrument for neutral and charged particle flows." *Rev. Sci. Instrum., 73*(10), 3500-3507 (2002).
[18] B. N. Breizman and A. V. Arefiev, "Single-Pass Ion Cyclotron Resonance Absorption." *Physics of Plasmas, 8*(3), 907-915 (2001).
[19] E. G. Shelley, R. D. Sharp, and R. G. Johnson, "Satellite observations of an ion acceleration mechanism." *Geophysical Research Letters, 3*(11), 654 (1976).
[20] R. D. Sharp, R. G. Johnson, and E. G. Shelley, "Observation of an ionospheric acceleration mechanism producing energetic (keV) ions primarily normal to the geomagnetic field direction." *Journal of Geophysical Research, 82*, 3324 (1977).
[21] F. S. Mozer, C. W. Carlson, M. K. Hudson et al., "Observations of paired electrostatic shocks in the polar shocks in the polar magnetosphere." *Physical Review Letters, 38,* 292 (1977).
[22] A. G. Ghielmetti, R. G. Johnson, R. D. Sharp et al., "The latitudinal, diurnal and altitudinal distributions of upward flowing energetic ions of ionospheric origin." *Geophysical Research Letters, 5,* 59 (1978).
[23] E. G. Shelley, "Heavy ions in the magnetosphere." *Space Science Reviews, 23,* 465 (1979).
[24] R. D. Sharp, R. G. Johnson, and E. G. Shelley, "Energetic particle measurements from within ionospheric structures responsible for auroral acceleration processes." *Journal of Geophysical Research, 84,* 480 (1979).
[25] H. L. Collin, R. D. Sharp, E. G. Shelley et al., "Some general characteristics of upflowing ion beams over the auroral zone and their relationship to auroral electrons." *Journal of Geophysical Research, 86,* 6820 (1981).
[26] E. A. Bering III, M. C. Kelley, and F. S. Mozer, "Observations of an intense field aligned thermal ion flow and associated intense narrow band electric field oscillations." *Journal of Geophysical Research, 80* (34), 4612-4620 (1975).
[27] E. A. Bering III and M. C. Kelley, "Observation of Electrostatic Ion Cyclotron Waves at the Boundary of an Auroral Arc." *EOS, Transactions, American Geophysical Union, 56,* 173 (1975).
[28] M. C. Kelley, E. A. Bering III, and F. S. Mozer, "Evidence that the electrostatic ion cyclotron instability is saturated by ion heating." *Physics of Fluids, 18,* 1590-1597 (1975).
[29] P. M. Kintner, M. C. Kelley, and F. S. Mozer, "Electrostatic hydrogen cyclotron waves near one earth radius altitude in the polar magnetosphere." *Geophysical Research Letters, 5,* 139 (1978).
[30] P. M. Kintner, M. C. Kelley, R. D. Sharp et al., "Simultaneous observations of energetic (keV) upstreaming ions and electrostatic hydrogen cyclotron waves." *Journal of Geophysical Research, 84,* 7201-7212 (1979).
[31] P. M. Kintner, "On the distinction between electrostatic ion cyclotron waves and ion cyclotron harmonic waves." *Geophysical Research Letters, 7,* 585 (1980).
[32] E. A. Bering III, "Apparent Electrostatic Ion Cyclotron Waves in the Diffuse Aurora." *Geophysical Research Letters, 10,* 647-650 (1983).
[33] E. A. Bering III, "The Plasma Wave Environment of an Auroral Arc, 1., Electrostatic Ion Cyclotron Waves in the Diffuse Aurora." *Journal of Geophysical Research, 89,* 1635-1649 (1984).
[34] [6]P. M. Kintner, W. Scales, J. Vago et al., "Harmonic H^+ gyrofequency structures in auroral hiss observed by high-altitude auroral sounding rockets." *Journal of Geophysical Research, 96*(A6), 9627-9638 (1991).
[35] J. P. Squire, F. R. Chang-Díaz, V. T. Jacobson et al., "Helicon plasma injector and ion cyclotron acceleration development in the VASIMR experiment." Presented at the *36th AIAA/ASME/SAE/ASEE Joint Propulsion Conference,* July17-19, Huntsville, Alabama, 2000.
[36] A. Petro, F. R. Chang-Díaz, A. V. Ilin et al., "Development of a space station-based flight experiment for the VASIMR magneto-plasma rocket." Presented at the *40th AIAA Aerospace Sciences Meeting and Exhibit,* 14-17 January, Reno, NV, 2002.
[37] F. R. Chang Díaz, "An overview of the VASIMR engine: High power space propulsion with RF plasma generation and heating." Presented at the *14th Topical Conference on Radio Frequency Power in Plasmas,* May 7-9, Oxnard, CA, 2001 (unpublished).
[38] R. W. Boswell, "Very efficient plasma generation by whistler waves near the lower hybrid frequency." *Plasma Phys. Control. Fusion, 26,* 1147 (1984).
[39] F. F. Chen, "Plasma ionization by helicon waves." *Plasma Physics and Controlled Fusion, 33*(4), 339-364 (1991).
[40] R. W. Boswell and F. F. Chen, "Helicons - The Early Years." *IEEE Transactions on Plasma Science, 25*(6), 1229-1244 (1997).
[41] R. W. Boswell and C. Charles, "The helicon double layer thruster." Presented at the *28th International Electric Propulsion Conference, IEPC 2003,* Toulouse, France, 2003.
[42] T. W. Glover, F. R. Chang-Díaz, V. T. Jacobson et al., "Ion Cyclotron Heating Results in the VASIMR VX-10." Presented at the *40th AIAA/ASME/SAE/ASEE Joint Propulsion Conference and Exhibit,* Fort Lauderdale, FL, 2004.
[43] E. A. Bering III, J. P. Squire, G. McCaskill et al., "Progress Toward the Development of a 50 kW VASIMR Engine." Presented at the *43rd AIAA Aerospace Sciences Meeting and Exhibit,* Reno, NV, 2005.

[44] E. A. Bering, III, M. Brukardt, J. P. Squire et al., "Recent Improvements In Ionization Costs And Ion Cyclotron Heating Efficiency In The VASIMR Engine." Presented at the *44th AIAA Aerospace Sciences Meeting and Exhibit,* Reno, NV, 2006.

[45] F. R. Chang Díaz, J. P. Squire, A. V. Ilin et al., "Early Results of ICRH Experiments in VX-10." *Bulletin of the American Physical Society DPP03,* RP1.138, 2003 (unpublished).

[46] E. A. Bering, III, F. R. Chang-Díaz, J. P. Squire et al., "Simulation of ion cyclotron heating in the auroral current region in the VASIMR", *Advances in Space Research,* (2007). (submitted to)

[47] V. I. Krassovsky, "Exploration of the upper atmosphere with the help of the third Soviet sputnik." *Proc. IRE, 47,* 289 (1959).

[48] E. C. Whipple, "The ion trap-results in "Exploration of the upper atmosphere with the help of the third Soviet sputnik"." *Proc. IRE, 47,* 2023 (1959).

[49] W. B. Hanson and D. D. McKibbin, "An ion-trap measurement of the ion-concentration profile above the F_2 peak." *Journal of Geophysical Research, 66,* 1667 (1961).

[50] L. W. Parker and E. C. Whipple, "Theory of spacecraft sheath structure, potential, and velocity effects on ion measurements by traps and mass spectrometers." *Journal of Geophysical Research, 75,* 4720-4733 (1970).

[51] W. B. Hanson, S. Sanatani, D. Zuccaro et al., "Plasma measurements with the retarding potential analyzer on OGO 6." *Journal of Geophysical Research, 75*(28), 5483-5501 (1970).

[52] W. B. Hanson, R. A. Heelis, R. A. Power et al., "The retarding potential analyzer for Dynamics Explorer-B." *Space Science Instruments, 5,* 503-510 (1981).

[53] S. Minami and Y. Takeya, "Ion temperature determination in the ionosphere by retarding potential analyzer aboard sounding rocket." *Journal of Geophysical Research, 87,* 713 (1982).

[54] J. P. Squire, F. R. Chang-Díaz, R. Bengtson et al., "A plasma diagnostic set for the study of a variable specific impulse magnetoplasma rocket." Presented at the *APS Division of Plasma Physics Meeting,* Pittsburg, PA, 1997 (unpublished).

[55] S.-L. Chen and T Sekiguchi, "Instantaneous Direct-Display System of Plasma Parameters by Means of Triple Probe." *Journal of Applied Physics, 36,* 2363 (1965).

[56] I. H. Hutchinson, *Principles of Plasma Diagnostics* (Cambridge University Press, Cambridge, 1987).

[57] M. D. Carter, F. W. Jr. Baity, G. C. Barber et al., "Comparing Experiments with Modeling for Light Ion Helicon Plasma Sources." *Physics of Plasmas, 9*(12), 5097-5110 (2002).

[58] R. L. Stenzel, R. Williams, R. Aguero et al., "Novel directional ion energy analyzer." *Review of Scientific Instruments, 53*(7), 1027-1031 (1982).

[59] R. L. Stenzel, W. Gekelman, N. Wild et al., "Directional velocity analyzer for measuring electron distribution functions in plasma," Review of Scientific Instruments 54, 1302-1310 (1983).